Density Functional Studies of Iron-Porphyrin Cation with Small Ligands X (X: O, CO, NO, O_2, N_2, H_2O, N_2O, CO_2)

Ayjamal Abdurahman*,† and Thomas Renger‡

Department of Chemistry, Centre for Research in Mass Spectrometry and Centre for Research in Earth and Space Science, York University, Toronto, Ontario, Canada M3J 1P3, and Institute of Chemistry and Biochemistry - Crystallography, Freie Universitaet Berlin, Takustr. 6, 14195 Berlin, Germany

Received: April 9, 2009; Revised Manuscript Received: July 1, 2009

Molecular structure of the iron porphyrin cation $[FeP]^+$ with small ligands X (X: O, CO, NO, O_2, N_2, H_2O, N_2O, CO_2) are studied employing density functional theory (DFT) methods with the exchange-correlation (XC) functionals OPBE and B3LYP using the LANL2DZ basis set. The relative spin state energies and bond dissociation energies of all of the complexes are presented at their optimized geometries. The low-spin ($S = 1/2$, $S = 0$) state is found to be the lowest energy states for the $[FePO]^+$, $[FePCO]^+$, and $[FePNO]^+$ complexes whereas the high-spin ($S = 5/2$) state has the lowest energy for the $[FePO_2]^+$ complex. The intermediate-spin ($S = 3/2$) state is found to be the lowest energy states for the $[FePN_2]^+$, $[FePH_2O]^+$, $[FePN_2O]^+$, and $[FePCO_2]^+$ complexes which exhibit the same relative spin-state energy ordering: ($S = 3/2$) < ($S = 5/2$) < ($S = 1/2$) as isolated $[FeP]^+$, and the Fe−ligand bonding is very weak. The calculated bond dissociation energy using the OPBE XC-functional method has shown the following order for the lowest energy spin state: $N_2O < CO_2 < N_2 < O_2 < H_2O < CO < NO < O$. This level of theory was previously shown to be the only DFT method capable of correctly predicting the spin ground state of iron compounds, and we find similar good performance of OPBE XC-functional in the current study.

I. Introduction

Enormous progress in molecular biology observed in recent years and high expectations connected to biotechnology resulted in increased interest for theoretical studies of biological molecules, particularly proteins. Many biological functions of proteins may now be successfully explained on a molecular level because of a careful analysis of both experimental and theoretical data. Iron porphyrins are subjects of active experimental and theoretical research because they serve as structural models for the active sites of heme proteins[1] and because of their importance in biology and catalysis.[2,3] Information about the electronic structure of the iron porphyrin, in particular, the spin state of the iron center, is crucial for understanding how hemoproteins perform their biological functions. An iron porphyrin complex is commonly occurring in the iron(II) or iron(III) oxidation state. A survey of literature data shows that Fe(III)P (P = porphyrin) complexes may exist as five- or six-coordinate species in which the 5d electrons of the central Fe^{III} ion can be arranged into three possible spin states, that is, the low-spin state ($S = 1/2$), intermediate-spin state ($S = 3/2$), and the high-spin state ($S = 5/2$).[4] One functionally important property is the relative energy of different spin states of a given metal complex. The accurate determination of the relative energies for the different low-energy spin states in the different oxidation states accessible to open-shell Fe(III)P and related complexes is still a computational challenge.[5] Most of the theoretical investigations have been done employing conventional density functional theory (DFT) methods.[6,7] The most widely used XC-functional is B3LYP.[8] The accuracy and deficiency of DFT with the B3LYP XC-functional are reviewed for transition metal complexes.[5,9] The relative energies of different spin states of metal complexes represent very challenging observables which can be used to test DFT accuracy.[10,11] Swart et al. reported a systematic investigation of a diversity of DFT functionals for predicting the spin ground state energies of iron complexes and have shown that the reliability of DFT methods for giving a proper description of relative spin state energies depends largely on the functional form of the exchange functional. The GGA exchange functional OPTX[12] in combination with the correlation functional PBE,[13] that is, OPBE, performs better than other functionals for spin-state splittings of iron complexes.[14,15] Furthermore, in a series of papers, Swart[16−18] reported the performance of the OPBE functional for the geometry optimization and also for spin state energies of iron containing complexes. Ghosh and co-workers[19] also demonstrated that the OPBE XC-functional is the most accurate for the overall description of the spin-state energetics of transition metal complexes.

We further assess the capability of the OPBE method in the present work by systematically investigating the ground state electronic structures, relative spin state energies, and bond dissociation energies of iron porphyrin cation $[FeP]^+$ with small ligands X (X: O, CO, NO, O_2, N_2, H_2O, CO_2, N_2O). For comparison, we also performed B3LYP calculations for all of the complexes. Through our DFT calculations, we want to provide a basis to understand the spin-structure relationships underlying the role of $[FeP]^+$ in the catalytic oxidation of atmospheric and organic molecules.

The organization of this paper is as follows. In section II, we present the details of the calculations. Section III deals with the results and discussions. Finally, we conclude this work with a summary in section IV.

* Corresponding author. Present address: Department of Chemical and Physical Sciences, University of Toronto Mississauga, 3359 Mississauga Road N, Mississauga, Ontario, Canada L5L 1C6.
† York University.
‡ Freie Universitaet Berlin.

10.1021/jp9032657 CCC: $40.75
Published on Web 07/20/2009

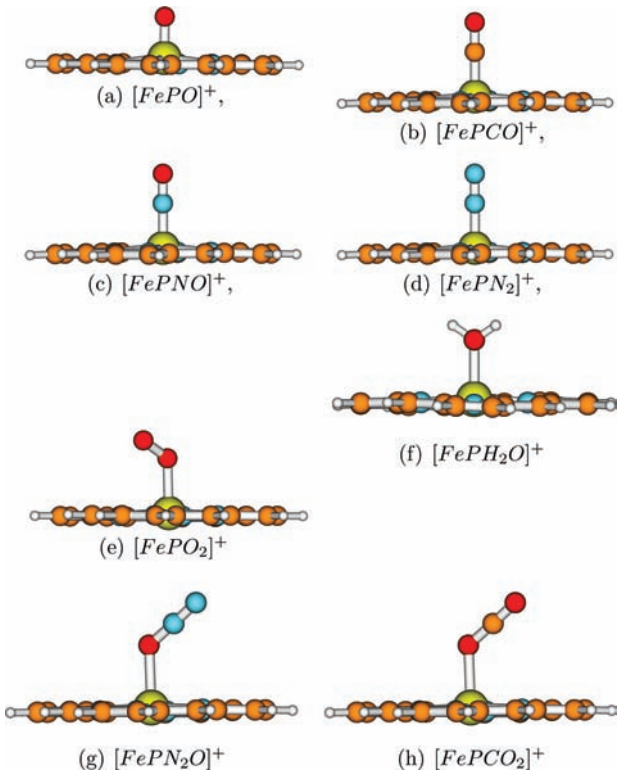

Figure 1. Model systems studied in the present work.

II. Methods and Computational Details

Our calculations were performed applying the OPBE and B3LYP XC functionals using the Dunning−Hay−Wadt basis sets LANL2DZ[20−23] as implemented in the Gaussian-03 suite.[24] The reference structures of all complexes are presented in Figure 1. Each complex consists of a planar porphyrin ring composed of four pyrrole rings and the ligand lie along an axis perpendicular to the plane of the porphyrin ring. As a ligand, we used the full oxygen derived molecule except N_2. Neutral forms of these CO ($S = 0$), NO ($S = 1/2$), O_2 ($S = 1$), N_2 ($S = 0$), H_2O ($S = 0$), CO_2 ($S = 0$), N_2O ($S = 0$) molecular ligands were used, resulting in a net charge on the complex of +1. Three spin (low, intermediate, and high-spin) states were considered for each model complex. Geometry optimizations were performed for $[FePO]^+$, $[FePCO]^+$, $[FePO_2]^+$, $[FePH_2O]^+$, $[FePN_2O]^+$, $[FePCO_2]^+$, and $[FePNO]^+$ complexes in low, intermediate, and high-spin states in the gas phase applying OPBE and B3LYP methods without any restrictions (symmetry, restraints, or constraints). Next, we have checked the stability of the wave function at the final geometry. The frequency calculations were performed to determine whether stationary points from geometry optimization calculations were local minima or saddle points and to determine the zero-point energies. Atomic charges are presented by the natural bond orbital (NBO) analysis.[25] The open shell systems were treated using unrestricted wave functions. The relative spin-state energies and the bond dissociation energies (BDE) of all of the complexes were calculated at their final optimized geometries. Zero-point energies were used to correct the BDE energies. To probe basis set effects on the relative spin state energies, we performed single-point energy calculations at the OPBE/LANL2DZ optimized geometries with a large (6−311++G**) basis set. In general, for all the complexes studied, the calculated S^2 values were in excellent agreement with the theoretically expected values for the high-spin and intermediate-spin states but not for the low-spin state. To account for spin contamination, the spin projected energy E_s is calculated by subtracting the energy contribution of the higher spin state E_{s+1} from the spin contaminated energy E_C with subsequent renormalization using the following equations:[26]

$$a = \frac{\langle S^2\rangle_c - s(s+1)}{2(s+1)} \quad (1)$$

$$E_s = \frac{E_c - aE_{s+1}}{1-a} \quad (2)$$

where $\langle S^2\rangle_C$ is the expectation value of S^2 obtained from the spin contaminated wave function and s is the total spin.

III. Results and Discussion

The spin multiplicities, structural parameters, and atomic charges are shown in Table 1. The spin multiplicities and calculated relative spin-state energies with OPBE and B3LYP XC-functional using the different basis sets are reported in Table 2. The bond dissociation energies (BDE) for the spin state with the lowest energy obtained by applying the OPBE and B3LYP XC-functionals are presented in Table 3. Remarkably, the OPBE optimized structures of all of the complexes except $[FePNO]^+$ for the low-spin state have shown that the porphyrin plane is strongly distorted by ruffling. The porphyrin deformation, especially the ruffling or saddling of the Fe(III)P complexes, was described recently in a review article[27] with an emphasis on the use of ^{1}H NMR, ^{13}C NMR, and ERP spectroscopy. However, as pointed out previously (see ref 27 and references therein) ruffling of the porphyrin plane is associated with a change in the electronic structures. In principle, there are two types of electronic ground states in low-spin Fe(III)P complexes. One is the commonly observed ground state with the $(d_{xy})^2(d_{xz},d_{yz})^3$ electron configuration and the other is the less common ground state with $(d_{xz},d_{yz})^4(d_{xy})^1$. On ruffling, the system prefers the less common $(d_{xz},d_{yz})^4(d_{xy})^1$ state. The unpaired electron in the d_{xy} orbital cannot mix with the porphyrin π-system if the porphyrin ring is planar, whereas upon ruffling of the porphyrin plane, the π orbitals of the porphyrin have in-plane components that can overlap with the d_{xy} orbital. This overlap allows the half-filled d_{xy} orbital of the iron to accept additional electron density from the porphyrin π orbitals in the ferric oxidation state. Below we discuss each complex separately.

A. Isolated Iron-Porphyrin Cation $[FeP]^+$. Geometry optimizations were carried out for three possible electronic configurations: low-spin ($S = 1/2$), intermediate-spin ($S = 3/2$), and high-spin ($S = 5/2$) states of the $[FeP]^+$ complex. As shown in Table 1, from OPBE geometry optimization the resulting lowest energy spin state is a quartet, and the relative spin-state energy order predicted for those spin states are ($S = 3/2$) < ($S = 5/2$) < ($S = 1/2$) which is in good agreement with the results reported in ref 28 in which they calculated the relative spin-state energy with *TZP* basis set using ADF program. The B3LYP method predicted also a ($S = 3/2$) ground state but switched the ordering of the doublet and sextet states, relative to OPBE. Geometrically, in each spin state, the four Fe−N bonds are equivalent, and there is no distortion in the Fe−4N plane. Both XC-functionals OPBE and B3LYP show that there is large spin contamination for the ($S = 1/2$) doublet state of $[FeP]^+$. The spin projection technique,[26] as discussed above, was used to obtain the results for the pure spin doublet.

TABLE 1: Spin Multiplicity (M_s) and Important Structural Parameters in (Å): Iron-Ligand Distance (d_X), Iron Displacement out of the Plane of the Porphyrin Nitrogens (d_P), Iron and Porphyrin Nitrogens Distance ($d_{Fe\text{-}4N}$), and Atomic Charges q_{Fe} of Fe

FeP^+	OPBe$_{(laN\prime2dz)}$				B3LYP$_{(laN\prime2dz)}$				SPIN
+X	d_X	d_P	$d_{Fe\text{-}4N}$	q_{Fe}	d_P	d_P	$d_{Fe\text{-}4N}$	q_{Fe}	M_s
$[FeP]^+$		0.0	2.00	1.09		0.0	2.01	1.16	2
		0.0	1.98	1.32		0.0	1.98	1.47	4
		0.0	2.03	1.70		0.0	2.07	1.46	6
$[FePO]^+$	1.61	*b*	2.00$^{(ave)}$	0.91	1.62	0.26	2.01	1.04	2
	1.62	0.22	2.07	0.94	1.62	0.25	2.01	1.04	4
	1.63	0.38	2.09	1.41	1.64	0.41	2.08	1.51	6
$[FePCO]^+$	1.69	*b*	1.96$^{(ave)}$	0.55	1.76	0.17	2.01	0.64	2
	2.34	0.12	1.99	1.20	1.77	0.20	2.02	0.67	4
	2.26	0.23	2.05	1.58	2.21	0.20	2.09$^{(ave)}$	1.47	6
$[FePNO]^+$	1.60	0.27	1.99	0.65	2.61	0.29	2.00	0.77	1
	1.75	0.0	1.98	0.91	2.24	0.0	1.98	1.32	3
	3.17	0.0	1.98	1.32	2.49	0.0	1.98	1.44	5
$[FePO2]^+$	2.19	*b*	1.98	1.20	2.17	0.0	2.01	1.16	4
	3.55	0.0	1.98	1.32	2.60	0.0	1.98	1.46	6
$[FePN2]^+$	1.84	*b*	1.99$^{(ave)}$	0.92	2.59[a]	0.0[a]	2.02[a]	1.15[a]	2
	2.83	0.0	1.98	1.31	2.46	0.06	1.99	1.44	4
	2.63	0.22	2.05	1.66	2.47	0.0	2.00	1.42	6
$[FePOH_2]^+$	2.10	*b*	2.00$^{(ave)}$	1.10	2.16	0.16	2.03	1.17	2
	2.20	0.2	1.99	1.31	2.12	0.21	2.00	1.46	4
	2.16	0.3	2.06	1.70	2.09	0.32	2.06	1.80	6
$[FePN_2O]^+$	3.76	0.0	2.00$^{(ave)}$	1.11	2.51	0.0	2.02	1.16	2
	3.51	0.0	1.98	1.33	2.33	0.0	1.99	1.45	4
	2.60	0.28	2.05	1.67	2.44	0.25	2.07$^{(ave)}$	1.49	6
$[FePCO_2]^+$	3.57	0.0	2.00	1.10	2.54[a]	0.0[a]	2.02[a]	1.17[a]	2
	2.91	0.0	1.98	1.34	2.36	0.14	1.99	1.47	4
	2.58	0.25	2.05	1.68	2.44[a]	0.20[a]	2.07[a]	1.62[a]	6

[a] Refers to optimized structure which has one imaginary frequency. [b] Refers to distorted ruffling structure.

TABLE 2: Spin Multiplicity, Relative Energies in (kcal/mol), and the Expectation Value of the Total Spin S^{2a}

	M_s	OPBe$_{(laN\prime2dz)}$	OPBe$_{(6\text{-}311++G^{**})}$	B3LYP$_{(laN\prime2dz)}$	$\langle S^2\rangle_C$
$[FeP]^+$	2	23.76, [26.4]	27.06	4.30	(1.86)
	4	0.0, [0.0]	0.0	0.0	(3.80)
	6	12.35, [13.0]	13.37	15.05	(8.76)
$[FePO]^+$	2	0.0	0.0	0.0	(1.53)
	4	0.50	3.08	0.15	(3.77)
	6	11.42	13.52	11.75	(8.82)
$[FePCO]^+$	2	0.0	0.0	0.0	(0.76)
	4	8.57	8.72	45.76	(3.80)
	6	17.18	17.78	6.77	(8.76)
$[FePNO]^+$	1	0.0	0.0	8.51	(0.0)
	3	8.32	9.95	0.0	(2.24)
	5	27.33	33.68	7.54	(6.05)
$[FePO_2]^+$	4	11.53	12.94	13.91	(4.33)
	6	0.0	0.0	0.0	(8.81)
$[FePN_2]^+$	2	19.58	18.53	9.05	(1.15)
	4	0.0	0.0	0.0	(3.80)
	6	10.28	11.50	42.21	(8.76)
$[FePH_2O]^+$	2	25.52, [26.6]	27.24	17.0	(1.55)
	4	0.0, [0.0]	0.0	0.0	(3.81)
	6	7.05, [8.4]	8.03	9.56	(8.76)
$[FePN_2O]^+$	2	26.99	30.12	10.19	(1.88)
	4	0.0	0.0	0.0	(3.80)
	6	10.6	12.66	10.17	(8.76)
$[FePCO_2]^+$	2	25.12	26.66	10.25	(1.87)
	4	0.0	0.0	0.0	(3.80)
	6	10.06	11.78	9.87	(8.76)

[a] Values in square brackets are taken from ref 28. Values in parentheses refer to computed $\langle S^2\rangle_c$ values (for pure spin states, the values are 0.75, 2.0, 3.75, 6.0, and 8.75 for a doublet, triplet, quartet, quintet, and sextet, respectively) using OPBE XC functional.

TABLE 3: Bond Dissociation Energies for the Lowest Spin State Energy in (kcal/mol) at 0 K and Spin Multiplicity (M_s)

	OPBe$_{(laN\prime2dz)}$	B3LYP$_{(laN\prime2dz)}$	M_s
$[FePO]^+$	69.43	46.53	2
$[FePCO]^+$	34.22	10.14	2
$[FePNO]^+$	49.29		1
		13.40	3
$[FePO_2]^+$	10.46	15.40	6
$[FePN_2]^+$	3.75	8.21	4
$[FePH_2O]^+$	14.45	23.15	4
$[FePN_2O]^+$	2.05	7.17	4
$[FePCO_2]^+$	2.48	7.49	4

B. Iron-Porphyrin Cation with Oxygen $[FePO]^+$. For the $[FePO]^+$ complex, the single oxygen atom is attached perpendicular to the porphyrin plane as shown in Figure 1. Similar to $[FeP]^+$, first, we performed geometry optimizations in the ($S = 1/2$), ($S = 3/2$), and ($S = 5/2$) states. Then, we calculated the relative spin state energy and bond dissociation energy. The optimized structures show that the Fe atom is about 0.2−0.4 Å out of the porphyrin plane, and the Fe-ligand distance is nearly not affected by the change in the spin state. The optimized structure (in Table 1) for the ($S = 1/2$) state at the OPBE level shows that the porphyrin plane is strongly distorted with ruffling. As for $[FeP]^+$, there is non-negligible spin contamination for the ($S = 1/2$) state, at both the OPBE and B3LYP levels. Both OPBE and B3LYP calculations predict that the lowest energy state has $S = 1/2$ which is very close in energy to the ($S = 3/2$) state differing by less than 1 kcal/mol. Calculations at both OPBE and B3LYP levels yield the same trend ($S = 1/2$) < ($S = 3/2$) < ($S = 5/2$) for the relative spin-state energies and also quantitatively agree quite well with each other (in Table 2). However, the calculated OPBE and B3LYP bond dissociation energies are quite different for the lowest energy spin ($S = 1/2$) state (in Table 3).

C. Iron-Porphyrin Cation with Carbon Monoxide $[FePCO]^+$. CO binding to Fe in the heme-CO system leads to a linear orientation of Fe−C−O which is well studied both experimentally[29] and theoretically.[30,31] In this work for the $[FePCO]^+$ complex, we considered a similar structure (as shown

Figure 1). Geometry optimization was performed for the (S = 1/2), (S = 3/2), and (S = 5/2) states. The (S = 1/2) state is found to be the lowest energy state at both the OPBE and the B3LYP levels. As shown in Table 1 for each spin state species, there is significant variation of the Fe-ligand distance and the Fe atom lies slightly out of the porphyrin plane, toward the CO group (by 0.1−0.2 Å). It is well-known that in the high-spin ground state of unligated heme the iron is situated (0.1−0.2 Å) above the porphyrin ring.[32,33] Remarkably, there is no spin contamination for the $[FePCO]^+$ complex in any spin state. As shown in Table 2 at the OPBE level, the order of stability of the spin state energies is (S = 1/2) < (S = 3/2) < (S = 5/2) whereas the B3LYP calculations switch the ordering of the relative spin-state energy. Here, the B3LYP behaves somewhat differently from OPBE and predicts subsequently higher relative spin-state energy for the (S = 3/2) state. In a previous theoretical study,[31] the ground state geometry was optimized, and the binding energy was calculated of the neutral (FePCO) complex applying molecular dynamics within the Car−Parrinello scheme. An optimized Fe-ligand distance of 1.69 Å and a binding energy of 26 kcal/mol were reported.[31] Interestingly, our calculations with OPBE give the same Fe-ligand distance and a somewhat higher bond dissociation energy (34.22 kcal/mol) for the cationic complex.

D. Iron-Porphyrin Cation with Nitric Oxide $[FePNO]^+$. It was reported that the binding of NO to an Fe(III) porphyrin leads to the formation of a low-spin diamagnetic (S = 0) mononitrosyl complex, in which the Fe−N−O unit takes a linear geometry.[34,35] There are a number of X-ray structures for the ferric NO-bound complex at different resolutions. In one structure, the Fe−N−O bond is linear; in another structure, the NO geometry is somewhat bent.[36] As shown in Figure 1, starting from linear conformation, we performed geometry optimization for the three possible spin states S = 0, S = 2, and S = 4. Whereas the OPBE XC-functional yields the lowest energy for the (S = 0) state, the B3LYP XC-functional predicts that lowest energy state has S = 2. Both methods obtain an interconversion from a linear to bend structure during geometry optimization for the S = 2 state, whereas a linear structure is obtained for the S = 0 and S = 4 states. In the bent structure the Fe−N−O bond angle is 146° and 126° at the OPBE and the B3LYP levels, respectively for the (S = 2) state. The OPBE optimized structure for the S = 2 state shows strong ruffling of the Fe−4N plane. The OPBE optimized structural parameters are in good agrement with those obtained with B3LYP for the S = 0 state but not for the S = 2 and the S = 4 states. Geometry optimization resulted in non-negligible spin contamination for the S = 2 state at the OPBE and B3LYP levels. However, for the S = 0 state B3LYP calculations do not find a stable minimum-energy structure. Furthermore, the B3LYP relative spin-state energy order S = 2 < S = 4 < S = 0 is completely different from that of OPBE which predicts the following order S = 0 < S = 2 < S = 4. For the present system, the optimized Fe-ligand distances 1.60 Å and 1.61 Å at the OPBE and the B3LYP levels, respectively, are much shorter than the bond length (1.69 Å) obtained by a Carr−Parrinello simulation on the neutral complex.[31] We note that an identical Fe-ligand bond length (1.61 Å) was reported for the $[FePNO]^+$ complex using the B3LYP/6-31G(d) in ref 34.

E. Iron-Porphyrin Cation with Dioxygen $[FePO_2]^+$. The ground state of the oxygen molecule is a triplet with two unpaired electrons. In binding O_2 to heme, the Fe−O−O unit is normally bent and takes a so-called end-on O_2 configuration.[31] Therefore, in this study, we optimized the structures of the $[FePO_2]^+$ complex for the different spin multiplicities. As a result, the lowest energy state is (S = 5/2), and the Fe−O−O angle is 144° and 156° at the OPBE and B3LYP levels, respectively. The Fe atom is positioned in the porphyrin plane. Our efforts to find a stable structure for the (S = 1/2) and (S = 3/2) states have been unsuccessful. The bond dissociation energy for the lowest energy state (S = 5/2) is 10 kcal/mol and 6.83 kcal/mol at the OPBE and B3LYP levels, respectively, which correlate well with previous theoretical results.[31]

F. Iron-Porphyrin Cation with Molecular Nitrogen $[FePN_2]^+$. Starting from the linear structure shown in Figure 1, we performed geometry optimization in the three spin states (S = 1/2), (S = 3/2), and (S = 5/2). The lowest energy spin state is found to be (S = 3/2) at both the OPBE and the B3LYP levels. In the resulting optimized structure for each spin state, the Fe atom is located in the porphyrin plane except for the (S = 5/2) state, for which there is a very small out of plane displacement (0.15 Å) at the OPBE level. Since the $[FePN_2]^+$ complex is isoelectronic to the $[FePCO]^+$ complex, the OPBE optimized structures obtained for each spin state are very similar. The most significant differences between different spin states are the iron-ligand distances which are significantly shorter in the (S = 1/2) state than in the (S = 3/2) and (S = 5/2) states. For each spin state species, the four FeP nitrogen distances are nearly equal. In contrast to OPBE, B3LYP yields an imaginary frequency for the optimized structure in the (S = 1/2) state, indicating problems to find the minimum.

G. Iron-Porphyrin Cation with Water $[FePH_2O]^+$. The H_2O molecule has a singlet (S = 0) ground state and is attached to the $[FeP]^+$ as shown in Figure 1. Similarly, we performed geometry optimization in the three spin states (S = 1/2), (S = 3/2), and (S = 5/2). From geometry optimization, the predicted lowest energy spin state is (S = 3/2) at both the OPBE and the B3LYP levels. The optimized structures for (S = 1/2), (S = 3/2), and (S = 5/2) states are not very similar. At the OPBE level, the Fe-ligand distance is longer in the sextet state than in the quartet and doublet states. At the B3LYP level, the Fe-ligand distance is longer in the doublet state than in the quartet and sextet states. At both levels, OPBE and B3LYP, the iron atom moves out of the Fe−4N plane by 0.1−0.3 Å for the (S = 1/2) state, and there are spin contaminations. At the OPBE level, the porphyrin ring is slightly distorted. Both methods yield the same trends: (S = 3/2) < (S = 5/2) < (S = 1/2) for the relative spin-state energy which is consistent with previous theoretical work.[28] The bond dissociation energies calculated by using the B3LYP XC functional agree with OPBE results for the (S = 1/2) state but are about 10 kcal/mol higher for the (S = 3/2) and (S = 5/2) states.

H. Iron-Porphyrin Cation with Nitrous Oxide $[FePN_2O]^+$. The ground state of the N_2O molecule is a singlet (S = 0) state and takes linear conformation.[37] For the starting geometry of the $[FePN_2O]^+$ complex, we considered a bent conformation of the Fe−N_2O unit. The optimized structures at the OPBE level show that there is an interconversion from the bent to the linear conformation for the (S = 1/2) and (S = 3/2) states whereas the optimization keeps the bent structure for the (S = 5/2) state with an angle of 138°. For each spin state conformations, there is no distortion of the Fe−4N plane. Fe lies in the Fe−4N plane for the (S = 1/2) and (S = 3/2) states and moves 0.28 Å out of the Fe−4N plane for the (S = 5/2) state.

I. Iron-Porphyrin Cation with Carbon Dioxide $[FePCO_2]^+$. CO_2 has no net dipole moment and consequently is not very reactive. It was known that the most stable coordination of CO_2 to metal cation takes the linear end-on conformation due to the

electrostatic(charge-quadruple) nature of the bonding.[38] As shown in Figure 1, we consider a bent conformation for the starting geometry of the $[FePCO_2]^+$ complex. The optimized structures applying the OPBE XC-functional shows that the stable coordination of CO_2 to $[FeP]^+$ is linear, and the predicted lowest energy spin state is ($S = 3/2$). There is no distortion of the Fe−4N plane in any spin state. Fe lies in the Fe−4N plane for the ($S = 1/2$) and ($S = 3/2$) states whereas it moves 0.25 Å out of the Fe−4N plane for the ($S = 5/2$) state. The relative spin-state energy ordering is ($S = 3/2$) < ($S = 5/2$) < ($S = 1/2$). The optimized structures at the B3LYP level for the ($S = 1/2$) and the ($S = 5/2$) states lead to an imaginary frequency indicating problems to find a stable minimum, whereas for the ($S = 3/2$) state the structure has a genuine minimum.

IV. Conclusions

We have studied different small molecules ligated to iron-porphyrin cation complexes using density functional theory at the OPBE and B3LYP levels. The optimized structures of all complexes except $[FePCO]^+$ have shown that the wave function suffers from non-negligible spin contamination in the ($S = 1/2$) spin state. An inspection of the tables reveal the following trends: (i) The relative energies of different spin (low, intermediate, high) states indicate that the ($S = 3/2$) state is the lowest energy state for the $[FeP]^+$, $[FePN_2]^+$, $[FePCO_2]^+$, $[FePN_2O]^+$, and $[FePH_2O]^+$ complexes. Furthermore, for the $[FePO]^+$ and $[FePCO]^+$ complexes, the ($S = 1/2$) spin state, and for the $[FePO_2]^+$ complex, the ($S = 5/2$) spin state, they are found to be the lowest energy states at both levels. The basis sets have virtually no effect on the overall ordering of relative spin state energies of all complexes. Our results show that for the $[FePNO]^+$ complex the B3LYP method has failed to predict the correct lowest spin state energy. Our theoretical investigations indicate the necessity of calculating various spin states since the spin state of the ground state is not directly apparent. (ii) The calculated bond dissociation energy using the OPBE XC-functional method has shown the following order for the lowest energy state: $N_2O < CO_2 < N_2 < O_2 < H_2O < CO < NO < O$. Because of the lack of experimental data, we cannot evaluate our results directly, but we hope these results will serve as a stimulus for experiments in the near future.

Acknowledgment. We would like to thank Professor Alan C. Hopkinson for comments and suggestions during the preparation of the manuscript. The author A. Abdurahman is grateful for computer resources support from ZEDAT at Free University Berlin.

References and Notes

(1) Iron Porphyrins; Lever, A. B., Gray, H. B., Eds.; *Physical Bioinorganic Chemistry Series*; Addison-Wesley: Reading, MA, 1983; Vols. 1−3.

(2) Dolphin, D.; Felton, R. H. *Acc. Chem. Res.* **1974**, *7*, 26.

(3) *The Porphyrin Handbook*; Kadish, K. Smith, K. Guilard, R., Eds.; Academic Press: London, 1999; Vols. I−VII.

(4) Scheidt, W. R.; Reed, Ch. A. *Chem. Rev.* **1981**, *81*, 543.

(5) Ghosh, A. *J. Biol. Inorg. Chem.* **2006**, *11*, 712.

(6) Parr, R. G. Yang, W. *Density Functional Theory of Atoms and Molecules*; Oxford University Press: New York, 1989.

(7) Koch, W. Holthausen, M. C. *A Chemist's Guide to Density Functional Theory*; Wiley-VCH; Weinheim, 2000.

(8) Becke, A. D. *J. Chem. Phys.* **1993**, *98*, 5648.

(9) Siegbahn, P. E. M. *J. Biol. Inorg. Chem.* **2006**, *11*, 695.

(10) Harvey, J. N. *Struct. Bonding (Berlin)* **2004**, *112*, 151.

(11) Harvey, J. N. *Annu. Rep. Prog. Chem., Sect. C: Phys. Chem.* **2006**, *102*, 203.

(12) Handy, N. C.; Kohen, A. J. *Mol. Phys.* **2001**, *99*, 403.

(13) Perdew, J. P.; Burke, K.; Ernzerhof, M. *Phys. Rev. Lett.* **1996**, *77*, 3865. Perdew, J. P.; Burke, K.; Ernzerhof, M. *Phys. Rev. Lett.* **1997**, *78*, 1396.

(14) Swart, M.; Groenhof, A. R.; Ehlers, A. W.; Lammertsma, K. *J. Phys. Chem A* **2004**, *108*, 5479.

(15) Swart, M.; Ehlers, A. W.; Lammertsma, K. *Mol. Phys.* **2004**, *102*, 2467.

(16) Swart, M. *Inorg. Chim. Acta* **2007**, *360*, 179.

(17) Swart, M. *J. Phys. Chem A* **2008**, *112*, 6384.

(18) Swart, M. *J. Chem. Theory Comput.* **2008**, *4*, 2057.

(19) Conradie, J.; Ghosh, A. *J. Chem. Theory Comput.* **2007**, *3*, 689.

(20) Dunning Jr, T. H. Hay, P. J. In *Modern Theoretical Chemistry*; Schaefer, H. F. III, Ed.; Vol. 3, Plenum: New York, 1976; pp 1−28.

(21) Hay, P. J.; Wadt, W. R. *J. Chem. Phys.* **1985**, *82*, 270.

(22) Wadt, W. R.; Hay, P. J. *J. Chem. Phys.* **1985**, *82*, 284.

(23) Hay, P. J.; Wadt, W. R. *J. Chem. Phys.* **1985**, *82*, 299.

(24) Frisch, M. J.; Trucks, G. W.; Schlegel, H. B.; Scuseria, G. E.; Robb, M. A.; Cheeseman, J. R.; Montgomery, Jr., J. A.; Vreven, T.; Kudin, K. N.; Burant, J. C.; Millam, J. M.; Iyengar, S. S.; Tomasi, J.; Barone, V.; Mennucci, B.; Cossi, M.; Scalmani, G.; Rega, N.; Petersson, G. A.; Nakatsuji, H.; Hada, M.; Ehara, M.; Toyota, K.; Fukuda, R.; Hasegawa, J.; Ishida, M.; Nakajima, T.; Honda, Y.; Kitao, O.; Nakai, H.; Klene, M.; Li, X.; Knox, J. E.; Hratchian, H. P.; Cross, J. B.; Bakken, V.; Adamo, C.; Jaramillo, J.; Gomperts, R.; Stratmann, R. E.; Yazyev, O.; Austin, A. J.; Cammi, R.; Pomelli, C.; Ochterski, J. W.; Ayala, P. Y.; Morokuma, K.; Voth, G. A.; Salvador, P.; Dannenberg, J. J.; Zakrzewski, V. G.; Dapprich, S.; Daniels, A. D.; Strain, M. C.; Farkas, O.; Malick, D. K.; Rabuck, A. D.; Raghavachari, K.; Foresman, J. B.; Ortiz, J. V.; Cui, Q.; Baboul, A. G.; Clifford, S.; Cioslowski, J.; Stefanov, B. B.; Liu, G.; Liashenko, A.; Piskorz, P.; Komaromi, I.; Martin, R. L.; Fox, D. J.; Keith, T.; Al-Laham, M. A.; Peng, C. Y.; Nanayakkara, A.; Challacombe, M.; Gill, P. M. W.; Johnson, B.; Chen, W.; Wong, M. W.; Gonzalez, C.; Pople, J. A.; Gaussian, Inc.: Wallingford, CT, 2004.

(25) Reed, A. E.; Curtiss, L. A.; Weinhold, F. *Chem. Rev.* **1988**, *88*, 899.

(26) Wittbrodt, J. M.; Schlegel, H. B. *J. Chem. Phys.* **1996**, *105*, 6574.

(27) Nakamura, M. *Coord. Chem. Rev.* **2006**, *250*, 2271.

(28) Groenhof, A. R.; Swart, M.; Ehlers, A. W.; Lammertsma, K. *J. Phys. Chem A* **2005**, *109*, 3411.

(29) Kachalova, G. S.; Pepov, A. N.; Bartunik, H. D. *Science* **1999**, *284*, 473. Vojtechovsky, J.; Schlichting, I.; Chu, K.; Sweet, R. M.; Brendzen, J. *Biophys. J.* **1999**, *77*, 2153.

(30) Spiro, T. G.; Kozlowski, P. M. *J. Am. Chem. Soc.* **1998**, *120*, 4524.

(31) Rovira, C.; Kunc, K.; Hutter, J.; Ballone, P.; Parrinello, M. *Int. J. Quantum Chem.* **1998**, *69*, 31.

(32) Mizutani, Y.; Kitagawa, T. *J. Phys. Chem B* **2001**, *105*, 10992.

(33) Hartmanndagger, H.; Zinser, S.; Komninos, P.; Schneider, R. T.; Nienhaus, G. U.; Parak, F. *Proc. Natl. Acad. Sci. U. S. A.* **1996**, *93*, 7013.

(34) Linder, D. P.; Rodgers, K. R.; banister, J.; Wyllie, G. R. A.; Ellison, M. K.; Scheidt, W. R. *J. Am. Chem. Soc.* **2004**, *126*, 14136.

(35) Jee, J. E.; Eigler, S.; Hampel, F.; Jux, N.; Wolak, M.; Zahl, A.; Stochel, G.; van Eldik, R. *Inorg. Chem.* **2005**, *44*, 7717.

(36) Roberts, S. A.; Weichsel, A.; Qiu, Y.; Shelnutt, J. A.; Walker, F. A.; Montfort, W. R. *Biochemistry.* **2001**, *40*, 11327.

(37) Wang, F.; Harcourt, R. D. *J. Phys. Chem A* **2000**, *104*, 1304.

(38) Sodupe, M.; Branchadell, V.; Rosi, M.; Bauschlicher, C. W., Jr. *J. Phys. Chem A* **1997**, *101*, 7854.

JP9032657